Invisibility and perfect reflectivity in waveguides with finite length branches

Lucas Chesnel, Sergei A Nazarov, Vincent Pagneux

Invisibility and perfect reflectivity in waveguides with finite length branches

Lucas Chesnel[1], Sergei A. Nazarov[2,3,4], Vincent Pagneux[5]

[1] INRIA/Centre de mathématiques appliquées, École Polytechnique, Université Paris-Saclay, Route de Saclay, 91128 Palaiseau, France;
[2] St. Petersburg State University, Universitetskaya naberezhnaya, 7-9, 199034, St. Petersburg, Russia;
[3] Peter the Great St. Petersburg Polytechnic University, Polytekhnicheskaya ul, 29, 195251, St. Petersburg, Russia;
[4] Institute of Problems of Mechanical Engineering, Bolshoy prospekt, 61, 199178, V.O., St. Petersburg, Russia;
[5] Laboratoire d'Acoustique de l'Université du Maine, Av. Olivier Messiaen, 72085 Le Mans, France.

E-mails: lucas.chesnel@inria.fr, srgnazarov@yahoo.co.uk, vincent.pagneux@univ-lemans.fr

(September 21, 2017)

Abstract. We consider a time-harmonic wave problem, appearing for example in water-waves theory, in acoustics or in electromagnetism, in a setting such that the analysis reduces to the study of a 2D waveguide problem with a Neumann boundary condition. The geometry is symmetric with respect to an axis orthogonal to the direction of propagation of waves. Moreover, the waveguide contains one branch of finite length. We analyse the behaviour of the complex scattering coefficients $\mathcal{R}$, $\mathcal{T}$ as the length of the branch increases and we exhibit situations where non reflectivity ($\mathcal{R} = 0$, $|\mathcal{T}| = 1$), perfect reflectivity ($|\mathcal{R}| = 1$, $\mathcal{T} = 0$) or perfect invisibility ($\mathcal{R} = 0$, $\mathcal{T} = 1$) hold. Numerical experiments illustrate the different results.

Key words. Waveguides, invisibility, non reflectivity, perfect reflectivity, scattering matrix, asymptotic analysis.

1 Introduction

Invisibility is an exciting topic in scattering theory. In the present article, we consider a time-harmonic waves problem in a 2D waveguide unbounded in one direction (say (Ox)) with a non-penetration (Neumann) boundary condition. This problem appears naturally in acoustics, in water-waves theory (for straight vertical walls and horizontal bottom) or in electromagnetism. In the waveguide geometry, at a given frequency, only a finite number of waves can propagate along the (Ox) axis. More precisely, the quantity of interest (the acoustic pressure, the velocity potential, ...) decomposes at $\pm\infty$ as the sum of a finite number of propagating waves plus an infinite number of exponentially decaying modes. All through the paper, we will assume that the frequency is small enough so that only one wave (the piston wave) can propagate in the 2D waveguide. To describe the scattering process of the incident piston wave coming from $-\infty$, classically one introduces two complex coefficients, namely the *reflection* and *transmission* coefficients, denoted $\mathcal{R}$ and $\mathcal{T}$, such that $\mathcal{R}$ (resp. $\mathcal{T}$) corresponds to the amplitude of the scattered field at $-\infty$ (resp. $+\infty$). According to the energy conservation, we have

$$|\mathcal{R}|^2 + |\mathcal{T}|^2 = 1. \tag{1}$$

In this work, we are interested in geometries where non reflectivity ($\mathcal{R} = 0$), perfect reflectivity ($\mathcal{T} = 0$) or perfect invisibility ($\mathcal{T} = 1$) occurs. Of course, due to the conservation of energy (1), perfect invisibility implies non reflectivity. The converse is wrong since we can have $|\mathcal{T}| = 1$ with $\mathcal{T} \neq 1$. In this case, the incident piston wave goes through the waveguide with a phase shift.

In this setting, examples of situations where quasi invisibility ($|\mathcal{R}|$ small or $|\mathcal{T} - 1|$ small) happens,

obtained via numerical simulations, exist in literature. We refer the reader to [38, 16] for water wave problems and to [1, 13, 36, 37, 19] for strategies based on the use of new "zero-index" and "epsilon near zero" metamaterials in electromagnetism (see [18] for an application to acoustic). Let us mention also that the problem of the existence of quasi invisible obstacles for frequencies close to the threshold frequency has been addressed in the analysis of the so-called Weinstein anomalies [40] (see e.g. [32, 21]).

As for the rigorous proof of existence of geometries where $\mathcal{R} = 0$ or $\mathcal{T} = 1$, literature is not very developed especially if we compare to what is available concerning the existence of *trapped modes* (see e.g. [39, 14, 15, 12, 22, 25, 35]). We remind the reader that trapped modes are non zero solutions to the homogeneous problem (2) which are exponentially decaying both at $\pm\infty$. Using a similar terminology, we can call *invisible modes* the solutions of (2) such that the scattered field is exponentially decaying both at $\pm\infty$ ($\mathcal{T} = 1$). Such a difference of treatment between trapped and invisible modes in literature is striking since the two notions seem to share similarities.

One approach to construct waveguides such that $\mathcal{R} = 0$ has been proposed in [5, 4] (see also [6, 2, 10, 11] for applications to other problems). The method consists in adapting the proof of the implicit functions theorem. More precisely, the idea is to observe that $\mathcal{R} = 0$ in the straight waveguide and then to make a well-chosen smooth perturbation of amplitude ε (small) in the boundary to keep $\mathcal{R} = 0$. As explained in [5], this strategy does not permit to impose $\mathcal{T} = 1$ (perfect invisibility) for waveguides with Neumann boundary conditions because the differential of $\mathcal{T}$ with respect to the deformation for the reference geometry is not onto in $\mathbb{C}$ (think to the assumptions of the implicit functions theorem). However, this problem was overcome in [3] where it is shown how to get $\mathcal{T} = 1$ (and not only $|\mathcal{T}| = 1$) working with singular perturbations (instead of smooth ones) made of thin rectangles. Let us mention that these types of techniques proposed in [27, 31] were used in [28, 30, 8, 29] in a similar context. In these works, the authors construct small (non necessarily symmetric) perturbations of the walls of a waveguide that preserve the presence of a trapped mode associated with an eigenvalue embedded in the continuous spectrum.

It is important to emphasize that the methods of the previous paragraph are perturbative methods. They require to start from a geometry where it is known that $\mathcal{R} = 0$ or/and $\mathcal{T} = 1$. In our case, this geometry is simply the reference (straight) waveguide. As a consequence, the technique cannot be used to construct waveguides where $\mathcal{T} = 0$ (perfect reflectivity). In this article, we propose to investigate another route allowing us to get $\mathcal{R} = 0$, $\mathcal{T} = 0$ and also $\mathcal{T} = 1$. It relies on two main ingredients: symmetries and asymptotic analysis for truncated waveguides. Interestingly, our approach provides examples of geometries where $\mathcal{R} = 0$ or $\mathcal{T} = 1$ which are not small perturbations of the reference waveguide. In our study, we will be led to consider scattering problems in T-shaped waveguides. Such problems have been considered in particular in [26, 34]. Let us mention also that this work shares connections with [9, 24, 7, 20]. In the latter papers, the authors investigate the presence of trapped modes (also called bound states) associated with eigenvalues embedded in the continuous spectrum in geometries similar to ours. Finally, note that in the present article, we deal only with the Neumann boundary conditions. However, Dirichlet waveguides can be treated similarly and analogous results would be obtained.

The paper is structured as follows. We begin by introducing the setting and notation in Section 2. The waveguide Ω_L is symmetric with respect to the (Oy) axis (perpendicular to the unbounded direction) and contains one vertical (along the (Oy) axis) branch of finite length $L - 1$. Using the symmetry, we decompose the problem into two sub-problems set in half-waveguides with different boundary conditions: one with Neumann boundary conditions, another with mixed (Dirichlet and Neumann) boundary conditions. Then, we compute an asymptotic expansion of the scattering coefficients $\mathcal{R}$, $\mathcal{T}$ as $L \to +\infty$ (the branch of finite length becomes longer and longer). This expansion depends on the number of propagating modes existing in the vertical branch of the unbounded T-shaped waveguide Ω_∞ obtained at the limit $L = +\infty$, and this number itself depends on the width ℓ of the vertical branch of Ω_∞. In Section 3, we focus our attention on small values of ℓ for which

only one propagating mode exists in the vertical branch of Ω_∞. In Section 4, we use the asymptotic expansions of the scattering coefficients to prove the existence of geometries where one has $\mathcal{R} = 0$ (non reflectivity) or $\mathcal{T} = 0$ (perfect reflectivity). In Section 5, we consider a larger value for the parameter ℓ such that two modes can propagate in the vertical branch of Ω_∞. In such cases, we show that the behaviour of the scattering coefficients as $L \to +\infty$ can be quite complex. Section 6 is dedicated to the proof of existence of waveguides where there holds $\mathcal{T} = 1$ (perfect invisibility). Finally, in Section 7 we provide numerical experiments illustrating the different results obtained in the paper and in Section 8, we give a brief conclusion.

2 Setting

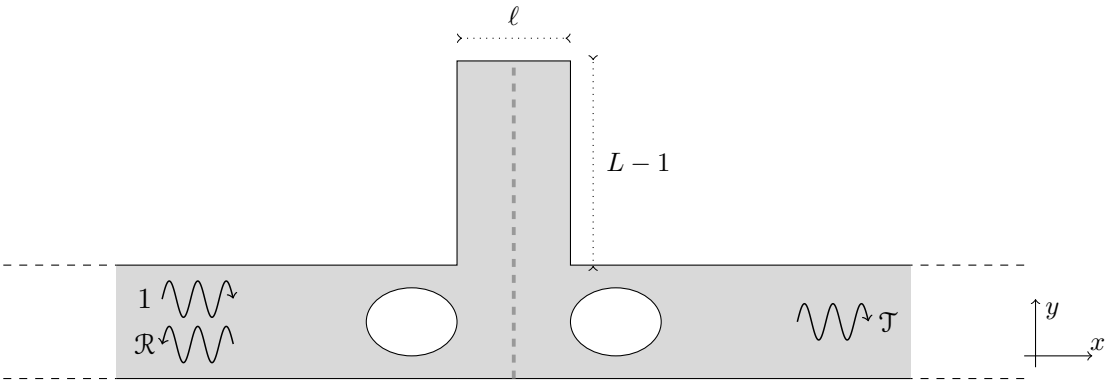

Figure 1: Example of geometry Ω_L. The vertical thick dashed line marks the axis of symmetry of the domain which will play a key role in the analysis.

For $\ell > 0$, $L > 1$, consider a connected open set $\Omega_L \subset \mathbb{R}^2$ (see Figure 1) which coincides with the region

$$\{(x, y) \in \mathbb{R} \times (0; 1) \ \cup \ (-\ell/2; \ell/2) \times [1; L)\}$$

outside a given ball centered at 0 of radius $d > 0$ (independent of ℓ, L). We assume that Ω_L is symmetric with respect to the (Oy) axis ($\Omega_L = \{(-x, y) \,|\, (x, y) \in \Omega_L\}$) and that its boundary $\partial\Omega_L$ is Lipschitz. We work in a rather academic geometry but other settings can be considered (see the discussion in Section 8). We assume that the propagation of time-harmonic waves in Ω_L is governed by the Helmholtz equation with Neumann boundary conditions

$$\left| \begin{array}{rcll} \Delta v + k^2 v & = & 0 & \text{in } \Omega_L \\ \partial_n v & = & 0 & \text{on } \partial\Omega_L. \end{array} \right. \tag{2}$$

In this problem, Δ denotes the 2D Laplace operator, k is the wavenumber and n stands for the normal unit vector to $\partial\Omega_L$ directed to the exterior of Ω_L. Moreover, v corresponds for example to the velocity potential in water-waves theory or to the pressure in acoustics. We assume that $k \in (0; \pi)$ so that k^2 is located between the first and second thresholds of the continuous spectrum $\sigma_c = [0; +\infty)$ of Problem (2) and we set

$$w^\pm(x, y) = e^{\pm ikx}/\sqrt{2k}.$$

In the following, $w^\pm$ will serve to define the incident and scattered fields. Introduce $\chi^+ \in \mathscr{C}^\infty(\mathbb{R}^2)$ (resp. $\chi^- \in \mathscr{C}^\infty(\mathbb{R}^2)$) a cut-off function that is equal to one for $x \geq 2\max(\ell, d)$ (resp. $x \leq -2\max(\ell, d)$) and to zero for $x \leq \max(\ell, d)$ (resp. $x \geq -\max(\ell, d)$). Now, the scattering problem we consider states

$$\left| \begin{array}{l} \text{Find } v \in \mathrm{H}^1_{\mathrm{loc}}(\Omega_L) \text{ such that } v - \chi^- w^+ \text{ is outgoing and} \\ \Delta v + k^2 v \ = \ 0 \quad \text{in } \Omega_L \\ \partial_n v \ = \ 0 \quad \text{on } \partial\Omega_L. \end{array} \right. \tag{3}$$

Here, $v - \chi^- w^+$ is outgoing means that there holds the decomposition (see the schematic picture 1)

$$v - \chi^- w^+ = \chi^- \mathcal{R}\, w^- + \chi^+ \mathcal{T}\, w^+ + \tilde{v} \tag{4}$$

with $\tilde{v} \in \mathrm{H}^1(\Omega_L)$ which is exponentially decaying at $\pm\infty$. One can prove that Problem (3) always admits a solution (see e.g. [33, Chap. 5, §3.3, Thm. 3.5 p.160]) which is possibly non uniquely defined if there is a trapped mode[1] at the wavenumber k. However, the reflection coefficient $\mathcal{R} \in \mathbb{C}$ and transmission coefficient $\mathcal{T} \in \mathbb{C}$ are always uniquely defined. They satisfy the energy conservation relation

$$|\mathcal{R}|^2 + |\mathcal{T}|^2 = 1$$

already written in (1). Of course $\mathcal{R}$ and $\mathcal{T}$ depend on the features of the geometry, in particular on L. In this work, we explain how to find some L such that $\mathcal{R} = 0$, $|\mathcal{T}| = 1$ (non reflectivity); $|\mathcal{R}| = 1$, $\mathcal{T} = 0$ (perfect reflectivity); or $\mathcal{R} = 0$, $\mathcal{T} = 1$ (perfect invisibility). To obtain such particular values for the scattering coefficients, we will use the fact that the geometry is symmetric with respect to the (Oy) axis. Define the half-waveguide

$$\omega_L := \{(x, y) \in \Omega_L \,|\, x < 0\}.$$

(see Figure 2, left). Introduce the problem with Neumann boundary conditions

$$\left| \begin{array}{rcll} \Delta u + k^2 u & = & 0 & \text{in } \omega_L \\ \partial_n u & = & 0 & \text{on } \partial\omega_L \end{array} \right. \tag{5}$$

as well as the problem with mixed boundary conditions

$$\left| \begin{array}{rcll} \Delta U + k^2 U & = & 0 & \text{in } \omega_L \\ \partial_n U & = & 0 & \text{on } \partial\omega_L \cap \partial\Omega_L \\ U & = & 0 & \text{on } \Sigma_L := \partial\omega_L \setminus \partial\Omega_L. \end{array} \right. \tag{6}$$

Problems (5) and (6) admit respectively the solutions

$$u = \chi^-(w^+ + r\, w^-) + \tilde{u}, \qquad \text{with } \tilde{u} \in \mathrm{H}^1(\omega_L), \tag{7}$$

$$U = \chi^-(w^+ + R\, w^-) + \tilde{U}, \qquad \text{with } \tilde{U} \in \mathrm{H}^1(\omega_L), \tag{8}$$

where r, $R \in \mathbb{C}$ are uniquely defined. Moreover, due to conservation of energy, one has

$$|r| = |R| = 1. \tag{9}$$

Briefly, let us explain how to show the latter identities. First, integrating by parts, one obtains

$$\int_{x=-\xi} \partial_n u\, \overline{u} - u\, \partial_n \overline{u}\, d\sigma = 0 \tag{10}$$

for $\xi > 0$ large enough. Here, we denote $\partial_n = -\partial_x$ at $x = -\xi$. Observing that the integral (10) does not depend on ξ, taking the limit $\xi \to +\infty$ and using the explicit representation (7), we get $|r| = 1$. Working analogously with U and exploiting (8) leads to $|R| = 1$.

Now, direct inspection shows that if v is a solution of Problem (3) then, we have $v(x, y) = (u(x, y) + U(x, y))/2$ in ω_L and $v(x, y) = (u(-x, y) - U(-x, y))/2$ in $\Omega_L \setminus \overline{\omega_L}$ (up possibly to a term which is exponentially decaying at $\pm\infty$ if there is a trapped mode at the given wavenumber k). We deduce that the scattering coefficients $\mathcal{R}$, $\mathcal{T}$ appearing in the decomposition (4) of v are such that

$$\mathcal{R} = \frac{r + R}{2} \qquad \text{and} \qquad \mathcal{T} = \frac{r - R}{2}. \tag{11}$$

Imagine that we want to have $\mathcal{R} = 0$ (non reflectivity). According to (11), we must impose $r = -R$. Relations (9) guarantee that for all $L > 1$, both r and R are located on the unit circle $\mathbb{S} := \{z \in \mathbb{C} \,|\, |z| = 1\}$. In the following, we will show that for ℓ, the width of the vertical branch of Ω_L, smaller

[1] We remind the reader that we call "trapped mode" a solution to Problem (2) which belongs to $\mathrm{H}^1(\Omega_L)$ (see [22] for more details).

than π/k, R tends to a constant $R_\infty \in \mathbb{S}$ while r runs continuously along $\mathbb{S}$ as $L \to +\infty$. This will prove the existence of L such that $r = -R$ and so $\mathcal{R} = 0$. This will also show that there is some L such that $r = R$ and, therefore, $\mathcal{T} = 0$ (perfect reflectivity). In order to obtain perfect invisibility, that is $\mathcal{T} = 1$, we must impose both $r = 1$ and $R = -1$. In other words, there is an additional constrain to satisfy and we will need to play with another degree of freedom. Here, we do not explain how to proceed, this will be the concern of Section 6. The important outcome of this discussion is that we will study the behaviour of r and R with respect to L going to $+\infty$. As one can imagine, this behaviour depends on the properties of the equivalents of Problems (5), (6) set in the limit geometry ω_∞ obtained from ω_L making $L \to +\infty$ (see Figure 2, right). More precisely, the number of propagating waves existing in the vertical branch of ω_∞ will play a key role in the analysis.

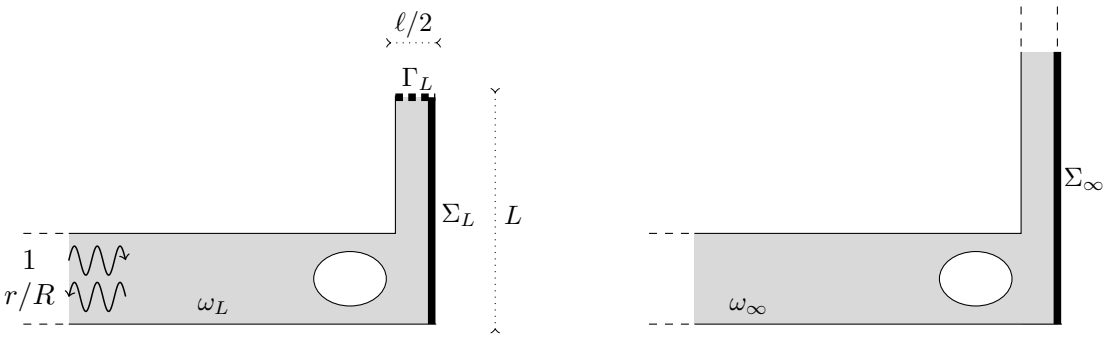

Figure 2: Domains ω_L (left) and ω_∞ (right).

3 Asymptotic expansion of the scattering coefficients as $L \to +\infty$

3.1 Half-waveguide problem with mixed boundary conditions

Consider the problem obtained from (6) making formally $L \to +\infty$:

$$\left|\begin{array}{rcll} \Delta U_\infty + k^2 U_\infty & = & 0 & \text{in } \omega_\infty \\ \partial_n U_\infty & = & 0 & \text{on } \partial\omega_\infty \cap \partial\Omega_\infty \\ U_\infty & = & 0 & \text{on } \Sigma_\infty := \partial\omega_\infty \setminus \partial\Omega_\infty. \end{array}\right. \tag{12}$$

Here Ω_∞ is the domain obtained from Ω_L with $L \to +\infty$. When $\ell \in (0; \pi/k)$, propagating modes in the vertical branch of ω_∞ for Problem (12) do not exist and we can show that (12) admits the solution

$$U_\infty = \chi^-(w^+ + R_\infty\, w^-) + \tilde{U}_\infty, \qquad \text{with } \tilde{U}_\infty \in \mathrm{H}^1(\omega_\infty),$$

where R_∞, such that $|R_\infty| = 1$, (work as in (9) to establish this identity), is uniquely defined. Then, proceeding as in [23, Chap. 5, §5.6], we can prove the expansion

$$U = U_\infty + \dots .$$

Here and in what follows, the dots correspond to a remainder which is exponentially small as $L \to +\infty$. Hence, we deduce

$$R = R_\infty + \dots . \tag{13}$$

More precisely, we can show that $R = R_\infty + O(e^{-\sqrt{k^2-(\pi/\ell)^2}L})$.

3.2 Half-waveguide problem with Neumann boundary conditions

Making $L \to +\infty$ in (5) leads to the problem

$$\left|\begin{array}{rcll} \Delta u_\infty + k^2 u_\infty & = & 0 & \text{in } \omega_\infty \\ \partial_n u_\infty & = & 0 & \text{on } \partial\omega_\infty. \end{array}\right. \tag{14}$$

When $\ell \in (0; 2\pi/k)$, one propagating mode exists in the vertical branch of ω_∞ for (14). Set

$$w_\circ^\pm(x,y) = e^{\pm iky}/\sqrt{k\ell}.$$

Problem (14) admits the solutions

$$\begin{array}{rcl} u_\infty^- & = & \chi^-(w^+ + r_\infty\, w^-) + \chi^\circ\, t_\infty\, w_\circ^+ + \tilde{u}_\infty^-, \\ u_\infty^\circ & = & \chi^-\, t_\infty^\circ\, w^- + \chi^\circ(w_\circ^- + r_\infty^\circ\, w_\circ^+) + \tilde{u}_\infty^\circ, \end{array} \tag{15}$$

where $\tilde{u}_\infty^-$, $\tilde{u}_\infty^\circ$ are functions in $\mathrm{H}^1(\omega_\infty)$ and where $\chi^\circ \in \mathscr{C}^\infty(\mathbb{R}^2)$ is such that $\chi^\circ = 0$ for $y \leq 1$, $\chi^\circ = 1$ for $y \geq 1+\delta$ ($\delta > 0$ is a constant). Observe for example that u_∞° is a solution in which an incident wave of unit amplitude travels in the negative $y-$direction. To obtain an asymptotic expansion of r as L goes to $+\infty$, let us compute an asymptotic expansion of u. For u, we make the ansatz [23, Chap. 5, §5.6]

$$u = u_\infty^- + a(L)\, u_\infty^\circ + \dots \tag{16}$$

where $a(L)$ is a gauge function, depending on L but not on (x,y), which has to be determined. On the segment $\Gamma_L := (-\ell/2; 0) \times \{L\}$, we find

$$\begin{array}{rcl} \partial_n u(x,L) & = & \partial_n u_\infty^-(x,L) + a(L)\, \partial_n u_\infty^\circ(x,L) + \dots \\ & = & ik\,(k\ell)^{-1/2}\,(\,t_\infty\, e^{ikL} + a(L)\,(-e^{-ikL} + r_\infty^\circ\, e^{ikL})\,) + \dots\ . \end{array}$$

Since $\partial_n u = 0$ on Γ_L, we take

$$a(L) = \frac{-t_\infty}{-e^{-2ikL} + r_\infty^\circ}. \tag{17}$$

In order $a(L)$ to be defined for all $L > 1$, we must have $|r_\infty^\circ| \neq 1$. Note that if $|r_\infty^\circ| = 1$, then $t_\infty^\circ = t_\infty = 0$. In that case, we choose $a(L) = 0$ and we can prove that $\mathcal{R} = r_\infty + \dots$. When $|r_\infty^\circ| \neq 1$, plugging expression (17) in (16) and identifying the main contribution of the terms of each side of the equality at $x = -\infty$, we get

$$r = r_{\mathrm{asy}}(L) + \dots \qquad \text{with} \quad r_{\mathrm{asy}}(L) := r_\infty - \frac{(t_\infty^\circ)^2}{-e^{-2ikL} + r_\infty^\circ}. \tag{18}$$

In (18), the subscript "$_{\mathrm{asy}}$" stands for "asymptotic" (and not "asymmetric"). As L tends to $+\infty$, the term $r_{\mathrm{asy}}(L)$ runs along the set

$$\{r_\infty - \frac{(t_\infty^\circ)^2}{z + r_\infty^\circ}\,|\,z \in \mathbb{S}\} \qquad \text{with} \quad \mathbb{S} = \{z \in \mathbb{C}\,|\,|z| = 1\}. \tag{19}$$

Using classical results concerning the Möbius transform, one finds that this set coincides with the circle centered at

$$r_\infty + \frac{(t_\infty^\circ)^2\, \overline{r_\infty^\circ}}{1 - |r_\infty^\circ|^2} \tag{20}$$

of radius

$$\frac{|t_\infty^\circ|^2}{1 - |r_\infty^\circ|^2}. \tag{21}$$

Using the relations $1 = |t_\infty^\circ|^2 + |r_\infty^\circ|^2$ and $r_\infty^\circ = -t_\infty^\circ \overline{r_\infty}/\overline{t_\infty^\circ}$[2], one can prove that the set defined in (19) is nothing else but the unit circle $\mathbb{S}$.

Since the dots in (18) correspond to terms which are exponentially decaying as L tends to $+\infty$, we infer that the coefficient r does not converge when $L \to +\infty$. Instead, asymptotically as $L \to +\infty$, it behaves like $r_{\mathrm{asy}}(L)$, *i.e.* it runs almost periodically along the unit circle $\mathbb{S}$. Since $|r| = 1$ for all $L \geq 1$, we deduce that r also runs (almost periodically) along $\mathbb{S}$ as $L \to +\infty$. The period, which is equal to π/k, tends to $+\infty$ when $k \to 0$.

[2] To derive this identity, work as in (9) with the integral $\int_{y=\xi} \partial_y u_\infty^- \overline{u_\infty^\circ} - u_\infty^- \partial_y \overline{u_\infty^\circ}\, d\sigma - (\int_{x=-\xi} \partial_x u_\infty^- \overline{u_\infty^\circ} - u_\infty^- \partial_x \overline{u_\infty^\circ}\, d\sigma)$.

3.3 Original problem

From Formula (11), we know that the coefficients $\mathcal{R}$, $\mathcal{T}$ appearing in the decomposition (4) of a solution to Problem (3) set in Ω_L satisfy $\mathcal{R} = (r+R)/2$ and $\mathcal{T} = (r-R)/2$. From the results of §3.1 and §3.2, we deduce that when $\ell \in (0;\pi/k)$, we have

$$\begin{aligned} \mathcal{R} &= \mathcal{R}_{\rm asy}(L) + \dots \qquad \text{with} \qquad \mathcal{R}_{\rm asy}(L) = (r_{\rm asy}(L) + R_\infty)/2, \\ \mathcal{T} &= \mathcal{T}_{\rm asy}(L) + \dots \qquad \text{with} \qquad \mathcal{T}_{\rm asy}(L) = (r_{\rm asy}(L) - R_\infty)/2. \end{aligned} \tag{22}$$

Here $r_{\rm asy}(L)$ is defined in (18). This shows that asymptotically, $\mathcal{R}$ (resp. $\mathcal{T}$) runs along a circle of radius $1/2$ centered at $R_\infty/2$ (resp. $-R_\infty/2$).

4 Non reflectivity and perfect reflectivity

We have $\mathcal{R} = (r+R)/2$ and $\mathcal{T} = (r-R)/2$ (Formula (11)). Moreover, for all $L \geq 1$, r and R are located on the unit circle $\mathbb{S}$. For a given $k \in (0;\pi)$, pick some $\ell \in (0;\pi/k)$ and assume that the coefficient r_∞ appearing in (15) satisfies $|r_\infty| \neq 1$. Then, the results of the previous section show that, as $L \to +\infty$, R tends to a constant while r runs continuously (and almost periodically) along $\mathbb{S}$. From the intermediate value theorem, we deduce that there is an infinite sequence of values $1 < L_1 < \dots < L_N < \dots$ such that for $L = L_n$, we have $r = -R$ and, therefore, $\mathcal{R} = 0$ for the chosen k. This provides examples of geometries where there holds non reflectivity. As $n \to +\infty$, we have

$$L_{n+1} - L_n = \pi/k + \dots,$$

where the dots denote exponentially small terms.

From this discussion, we also infer that there is another infinite sequence of values $1 < \boldsymbol{L}_1 < \dots < \boldsymbol{L}_N < \dots$ such that for $L = \boldsymbol{L}_n$, there holds $r = R$ and, therefore, $\mathcal{T} = 0$. This provides examples of geometries where we have perfect reflectivity. As $n \to +\infty$, again we have $\boldsymbol{L}_{n+1} - \boldsymbol{L}_n = \pi/k + \dots$.

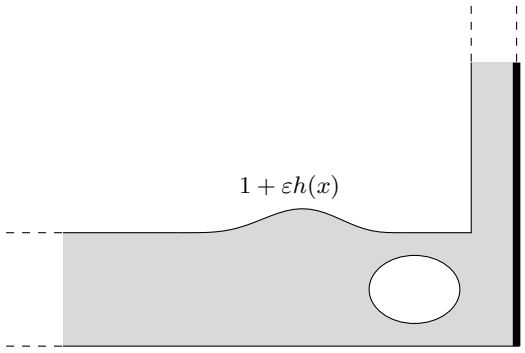

Figure 3: Domain $\omega_\infty^\varepsilon$ obtained as a perturbation of ω_∞.

Note that the assumption $|r_\infty| \neq 1$ is not restrictive. Indeed, if $|r_\infty| = 1$ for some ℓ, we can make a small perturbation of order ε as described in Figure 3. More precisely, for some function $h \in \mathscr{C}_0^\infty(\mathbb{R})$ supported in $(-\infty; -\max(\ell/2, d))$ and some ε small enough, define the domain $\omega_\infty^\varepsilon$ which coincides with ω_∞ for $x \geq -\max(\ell/2, d))$ and with

$$\{(x,y) \in \mathbb{R}^2 \,|\, x \in (-\infty;0),\ 0 < y < 1 + \varepsilon h(x)\}$$

for $x \geq -\max(\ell/2, d))$. Denote r_∞^ε the equivalent of the coefficient r_∞ in the geometry $\omega_\infty^\varepsilon$ instead of ω_∞. We can prove that

$$r_\infty^\varepsilon = r_\infty - \frac{\varepsilon}{2} \int_{-\infty}^{-\ell/2} \partial_x h(x)\, u_\infty^-(x) w^+(x)\, dx + O(\varepsilon^2).$$

Making the perturbation far away from zero so that , $u_\infty^- \approx w^+ + r_\infty\, w^-$, we can find some h and some ε so that $|r_\infty^\varepsilon| \neq 1$. Then the geometry Ω_L^ε where we have non reflectivity or perfectly reflectivity is defined from $\omega_L^\varepsilon := \{(x,y) \in \omega_\infty^\varepsilon \,|\, y < L\}$ thanks to the symmetry with respect to (Oy).

5 Two propagating modes in the vertical strip

In §3.3, we computed an asymptotic expansion of the coefficients $\mathcal{R}$, $\mathcal{T}$ as $L \to +\infty$ when $\ell \in (0; \pi/k)$. In this case, one propagating mode exists in the vertical branch of Ω_∞ for the initial problem (3).

When $\ell \in (\pi/k; 2\pi/k)$, the main change compare to what has been done in Sections 3, 4 is that one propagating mode exists in the vertical branch of ω_∞ for Problem (12) with mixed boundary conditions. Set

$$w_\bullet^\pm(x,y) = (\alpha\ell/2)^{-1/2} e^{\pm i\alpha y} \sin(\pi x/\ell), \quad \alpha = \sqrt{k^2 - (\pi/\ell)^2}.$$

Problem (12) admits the solutions

$$\begin{array}{rcl} U_\infty^- & = & \chi^-(w^+ + R_\infty\, w^-) + \chi^\circ\, T_\infty\, w_\bullet^+ + \tilde{U}_\infty^-, \\ U_\infty^\bullet & = & \chi^-\, T_\infty^\bullet\, w^- + \chi^\circ(w_\bullet^- + R_\infty^\bullet\, w_\bullet^+) + \tilde{U}_\infty^\bullet, \end{array} \tag{23}$$

where $\tilde{U}_\infty^-$, $\tilde{U}_\infty^\bullet$ are functions in $\mathrm{H}^1(\omega_\infty)$. To obtain an asymptotic expansion of R as L goes to $+\infty$, we will work exactly as in §3.2 where we derived an expansion for r. We first compute an asymptotic expansion of U. For U, we make the ansatz

$$U = U_\infty^- + A(L)\, U_\infty^\bullet + \dots \tag{24}$$

where $A(L)$ is a gauge function, depending on L but not on (x,y), which has to be determined. On the segment $\Gamma_L = (-\ell/2; 0) \times \{L\}$, we find

$$\begin{array}{rcl} \partial_n U(x,L) & = & \partial_n U_\infty^-(x,L) + A(L)\, \partial_n U_\infty^\bullet(x,L) + \dots \\ & = & i\alpha\, (\alpha\ell/2)^{-1/2}\, (\, T_\infty\, e^{i\alpha L} + A(L)\, (-e^{-i\alpha L} + R_\infty^\bullet\, e^{i\alpha L})\,) + \dots\ . \end{array}$$

Since $\partial_n U = 0$ on Γ_L, we take

$$A(L) = \frac{-T_\infty}{-e^{-2i\alpha L} + R_\infty^\bullet}. \tag{25}$$

In order $A(L)$ to be defined for all $L > 1$, we must have $|R_\infty^\bullet| \neq 1$. Note that if $|R_\infty^\bullet| = 1$, then $T_\infty^\bullet = T_\infty = 0$. In that case, we choose $A(L) = 0$ and we can prove that $R = R_\infty + \dots$. When $|R_\infty^\bullet| \neq 1$, plugging expression (25) in (24) and identifying the main contribution of the terms of each side of the equality at $x = -\infty$ yields

$$R = R_{\mathrm{asy}}(L) + \dots \qquad \text{with} \quad R_{\mathrm{asy}}(L) := R_\infty - \frac{(T_\infty^\bullet)^2}{-e^{-2i\alpha L} + R_\infty^\bullet}. \tag{26}$$

Working as in (20)–(21), we can prove that the term $R_{\mathrm{asy}}(L)$ runs along the unit circle as L tends to $+\infty$.

Coupling these results with the ones obtained in §3.2, we deduce that when $\ell \in (\pi/k; 2\pi/k)$, the scattering coefficients for Problem (3) set in Ω_L admit the asymptotic expansion

$$\begin{array}{lll} \mathcal{R} = \mathcal{R}_{\mathrm{asy}}(L) + \dots & \text{with} & \mathcal{R}_{\mathrm{asy}}(L) = (r_{\mathrm{asy}}(L) + R_{\mathrm{asy}}(L))/2, \\ \mathcal{T} = \mathcal{T}_{\mathrm{asy}}(L) + \dots & \text{with} & \mathcal{T}_{\mathrm{asy}}(L) = (r_{\mathrm{asy}}(L) - R_{\mathrm{asy}}(L))/2. \end{array} \tag{27}$$

Here $r_{\mathrm{asy}}(L)$, $R_{\mathrm{asy}}(L)$ are respectively defined in (18), (26). In §3.3, where $\ell \in (0; \pi/k)$ so that only one propagating mode exists in the vertical branch of Ω_∞, we gave an explicit characterization of the sets (circles of radius 1/2 passing through zero) which are described by $\mathcal{R}_{\mathrm{asy}}(L)$, $\mathcal{T}_{\mathrm{asy}}(L)$ as L goes to $+\infty$. In the present situation, this seems much less simple and numerical experiments in §7.2 show that the behaviour of $\mathcal{R}_{\mathrm{asy}}(L)$, $\mathcal{T}_{\mathrm{asy}}(L)$ when $L \to +\infty$ can be quite complicated. Let us just consider cases where there are $m, n \in \mathbb{N}^* := \{1, 2, \dots\}$, with $m > n$, such that

$$k = \alpha\, \frac{m}{n} \qquad \Leftrightarrow \qquad \ell = \frac{\pi}{k}\, \frac{m}{\sqrt{m^2 - n^2}}\,. \tag{28}$$

This boils down to assume that k/α is a rational number. Define $z = e^{-2i\alpha L/n}$. As $L \to +\infty$, $\mathcal{R}_{\rm asy}(L)$, $\mathcal{T}_{\rm asy}(L)$ run respectively along the sets

$$\mathcal{S}_{\mathcal{R}} := \Big\{ \frac{1}{2}\Big(r_\infty - \frac{(t_\infty^\circ)^2}{-z^m + r_\infty^\circ}\Big) - \frac{1}{2}\Big(R_\infty - \frac{(T_\infty^\bullet)^2}{-z^n + R_\infty^\bullet}\Big) \,|\, z \in \mathbb{S} \Big\},$$
$$\mathcal{S}_{\mathcal{T}} := \Big\{ \frac{1}{2}\Big(r_\infty - \frac{(t_\infty^\circ)^2}{-z^m + r_\infty^\circ}\Big) + \frac{1}{2}\Big(R_\infty - \frac{(T_\infty^\bullet)^2}{-z^n + R_\infty^\bullet}\Big) \,|\, z \in \mathbb{S} \Big\}.$$

In other words, $\mathcal{R}_{\rm asy}(L)$, $\mathcal{T}_{\rm asy}(L)$ run $n\pi/\alpha$-periodically along the close curves $\mathcal{S}_{\mathcal{R}}$, $\mathcal{S}_{\mathcal{T}}$ in the complex plane. Moreover, for any $L_\star > 1$, for $L \in [L_\star; L_\star + n\pi/\alpha]$, $L \mapsto r_{\rm asy}(L)$ (resp. $L \mapsto R_{\rm asy}(L)$) runs continuously m times (resp. n times) along $\mathbb{S}$. Therefore, according to the intermediate value theorem, we know that there exist at least $m-n$ values of $L \in [L_\star; L_\star + n\pi/\alpha]$ such that $R_{\rm asy}(L) = r_{\rm asy}(L)$ and $m-n$ other values of $L \in [L_\star; L_\star + n\pi/\alpha]$ such that $R_{\rm asy}(L) = -r_{\rm asy}(L)$. Since $\mathcal{R} = (r_{\rm asy}(L) + R_{\rm asy}(L))/2 + \dots$, and $\mathcal{T} = (r_{\rm asy}(L) - R_{\rm asy}(L))/2 + \dots$, we infer that there are some constants $\alpha(L_\star) \le 0$ and $\beta(L_\star) \ge 0$ (exponentially small with respect to $L_\star$) such that $L \mapsto \mathcal{R}$ and $L \mapsto \mathcal{T}$ vanish at least $m-n$ times in $[L_\star + \alpha(L_\star); L_\star + n\pi/\alpha + \beta(L_\star)]$. This provides examples of geometries where we have non reflectivity or perfect reflectivity with $\ell \in (\pi/k; 2\pi/k)$.

When k/α is not a rational number, since $r_{\rm asy}(L)$ runs faster than $R_{\rm asy}(L)$ along the unit disk (because $k > \alpha_\bullet$), we can still conclude that there are some L such that $\mathcal{R} = 0$ or $\mathcal{T} = 0$. However, there is no longer periodicity (or more precisely, approximate periodicity).

6 Perfect invisibility

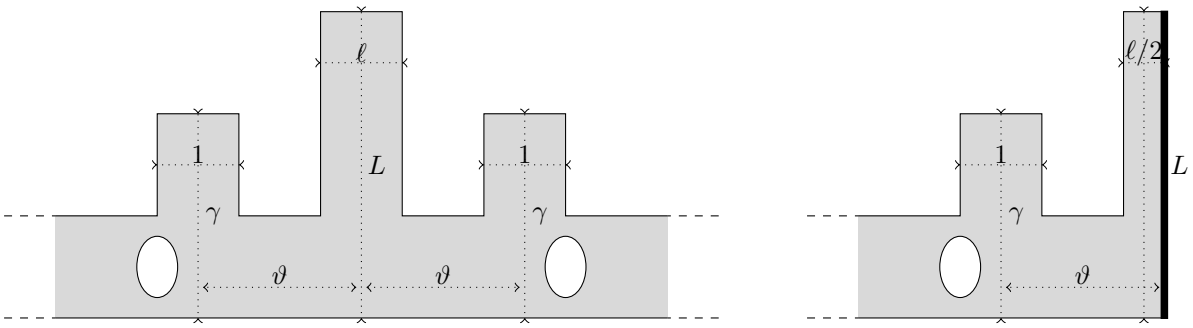

Figure 4: Domains Ω_L^γ (left) and ω_L^γ (right).

Up to now, we have explained how to impose $\mathcal{R} = 0$ (non reflectivity) or $\mathcal{T} = 0$ (perfect reflectivity). In this section, we show how to get $\mathcal{T} = 1$ (perfect invisibility). Since $\mathcal{T} = (r - R)/2$ (Formula (11)), we must impose both $r = 1$ and $R = -1$. To proceed, we work in a new geometry Ω_L^γ (see Figure 4, left) which coincides with the region

$$\{(x,y) \in \mathbb{R} \times (0;1) \ \cup \ (-\ell/2; \ell/2) \times [1; L) \ \cup \ (\pm\vartheta - 1/2; \pm\vartheta + 1/2) \times [1; \gamma)$$

outside a bounded domain. Again we assume that Ω_L^γ is symmetric with respect to the (Oy) axis ($\Omega_L^\gamma = \{(-x,y) \,|\, (x,y) \in \Omega_L^\gamma\}$), connected and that its boundary is Lipschitz. Here $\gamma > 1$ and $\vartheta > \ell/2 + 0.5$. The parameter ϑ is chosen only so that the central branch is distinct from the two others. Let ω_L^γ refer to the half-waveguide such that $\omega_L^\gamma := \{(x,y) \in \Omega_L^\gamma \,|\, x < 0\}$ (Figure 4 right). Again, denote $\mathcal{R}$, $\mathcal{T}$ (resp. r, R) the scattering coefficients for Problem (3) (resp. for Problems (5), (6)) set in Ω_L^γ (resp. ω_L^γ). For $\ell \in (0; \pi/k)$ and a given $\gamma > 0$, as explained in §3.1, R tends to a constant R_∞ located on the unit circle $\mathbb{S}$. Making $\gamma \to +\infty$, we can prove as in §3.2 that R_∞ runs continuously along $\mathbb{S}$. This allows one to deduce that there is $\gamma = \gamma_\infty$ such that $R_\infty = -1$. Then, tuning γ into $\gamma(L)$, with $\gamma(L)$ exponentially close to γ_∞, we can impose $R = -1$ for all L sufficiently large. On the other hand, the coefficient r runs along $\mathbb{S}$ as $L \to +\infty$. Therefore, almost periodically, we have $r = 1$ and $R = -1$ so that $\mathcal{T} = 1$.

7 Numerical results

We give here illustrations of the results obtained in the previous section. For given $\ell > 0$, $L > 1$, we approximate numerically the solution of Problem (3) with a P2 finite element method set in the bounded domain $\Omega_b := \{(x, y) \in (-8; 8) \times (0; 1) \cup (-\ell/2; \ell/2) \times [1; L)\}$ (see Figure 13). We emphasize that we work in a very simple geometry but other waveguides, for example with voids as depicted in Figure 1, can be considered. In particular in this geometry, one can use analytic methods (see e.g. [17]) instead of finite element techniques. At $x = \pm 8$, a Dirichlet-to-Neumann map with 20 modes serves as a transparent boundary condition. From the numerical solution v_h, we deduce approximations $\mathcal{R}_h$, $\mathcal{T}_h$ of the scattering coefficients $\mathcal{R}$, $\mathcal{T}$ defined in (4) (here h refers to the mesh size). Then, we display the behaviour of $\mathcal{R}_h$, $\mathcal{T}_h$ with respect to L. For the numerics, the wavenumber k is set to $k = 0.8\pi \in (0; \pi)$.

7.1 Case 1: one propagating mode exists in the vertical branch of Ω_∞

First, we investigate the situation of §3.3 where $\ell \in (0; \pi/k)$. To obtain the results of Figures 5-6, we take $\ell = 1 \in (0; \pi/k)$. In Figure 5, we observe that, asymptotically as $L \to +\infty$, the coefficients $\mathcal{R}_h$, $\mathcal{T}_h$ run along circles. This is coherent with what was derived in (22). Figure 6 confirms that the coefficients $\mathcal{R}$, $\mathcal{T}$ are asymptotically periodic with respect to $L \to +\infty$. More precisely, in (22), we found that the period must be equal to $\pi/k = 1.25$, which is more or less what is obtained in Figure 6. Figure 6 also confirms that, periodically, $\mathcal{R}$, $\mathcal{T}$ are equal to zero.

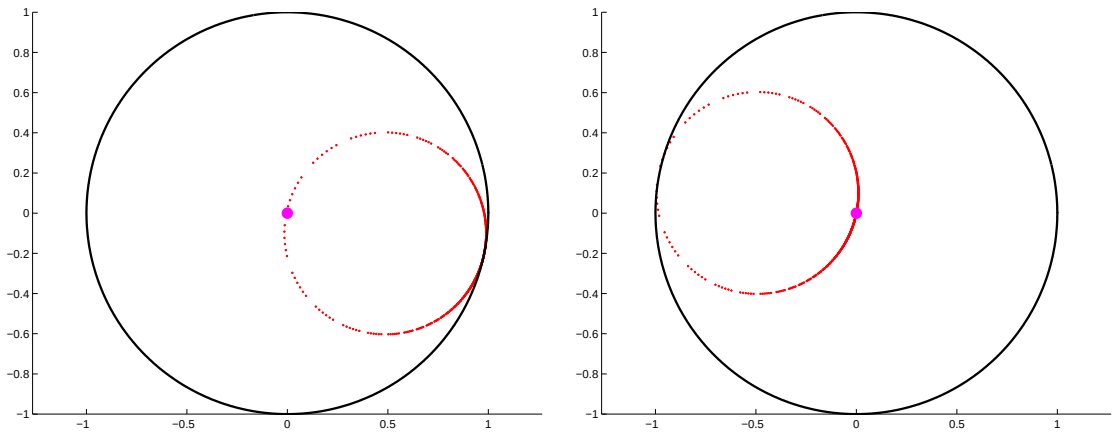

Figure 5: Coefficients $\mathcal{T}_h$ (left) and $\mathcal{R}_h$ (right) for $\ell = 1 \in (0; \pi/k)$ and $L \in (2; 10)$. Note that due to the conservation of energy, the coefficients $\mathcal{R}$, $\mathcal{T}$ are located inside the unit disk.

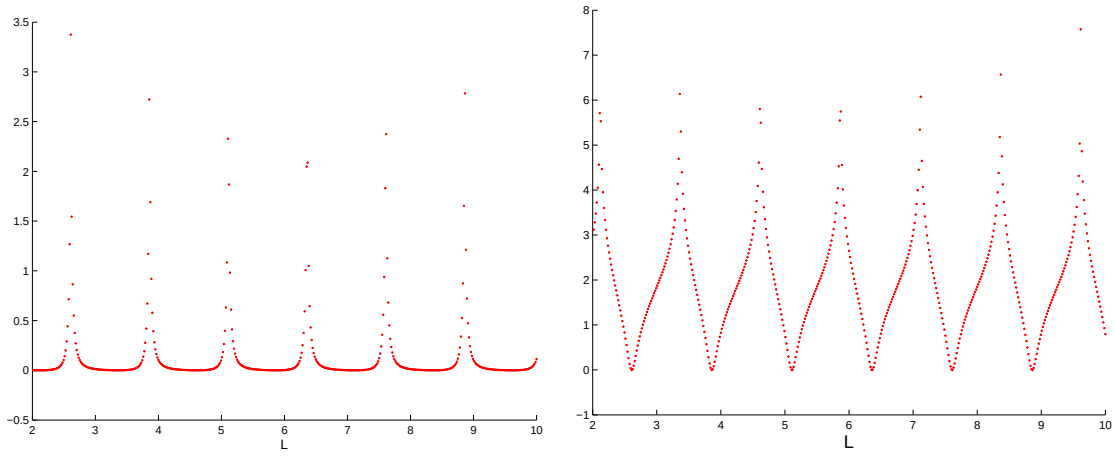

Figure 6: Curves $L \mapsto -\ln|\mathcal{T}_h|$ (left) and $L \mapsto -\ln|\mathcal{R}_h|$ (left) for $\ell = 1$.

In the next series of experiments, we study the properties of the asymptotic circles $\{\mathcal{T}_{\text{asy}}(L) \,|\, L \in (1; +\infty)\}$ and $\{\mathcal{R}_{\text{asy}}(L) \,|\, L \in (1; +\infty)\}$ defined in (22) with respect to the width $\ell \in (0; \pi/k)$ of the

vertical branch. For each $\ell \in (0;\pi/k)$, we showed that $\{\mathcal{T}_{\text{asy}}(L)\,|\,L \in (1;+\infty)\}$ (resp. $\{\mathcal{R}_{\text{asy}}(L)\,|\,L \in (1;+\infty)\}$) is a circle of radius $1/2$ centered at $-R_\infty/2$ (resp. $R_\infty/2$). Therefore, numerically it suffices, for all $\ell \in (0;\pi/k)$, to compute an approximation of the coefficient R_∞ solving Problem (12) set in ω_∞. The results are displayed in Figure 7. If we take $\ell = 1$, we observe that the obtained circles coincide with the ones of Figure 5.

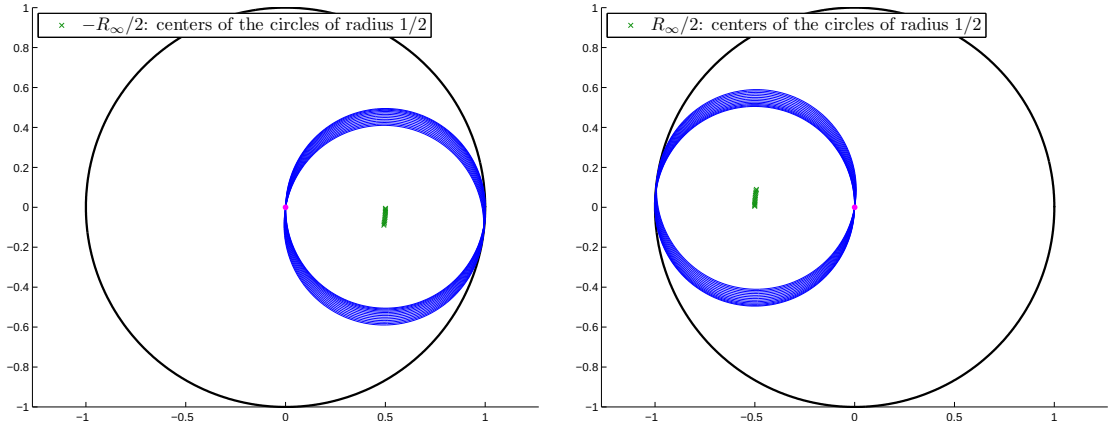

Figure 7: Asymptotic circles with respect to $\ell \in (0;\pi/k)$. For each ℓ, there is one circle. Left: $\{\mathcal{T}_{\text{asy},\,h}(L)\,|\,L \in (1;+\infty)\}$, right: $\{\mathcal{R}_{\text{asy},\,h}(L)\,|\,L \in (1;+\infty)\}$.

7.2 Case 2: two propagating modes exist in the vertical branch of Ω_∞

Now, we consider the case $\ell \in (\pi/k;2\pi/k)$ which has been studied in Section 5. In Figures 8 left and 9 left, we display the behaviour of $\mathcal{T}_h$, $\mathcal{R}_h$ for $\ell = 1.4$ and $L \in (2;10)$. Independently, numerically we can compute the coefficients r_∞, t_∞, r_∞° (resp. R_∞, T_∞, $R_\infty^\bullet$) appearing in (15) (resp. (23)). Hence, we can approximate the coefficients $\mathcal{R}_{\text{asy}}(L)$, $\mathcal{T}_{\text{asy}}(L)$ defined in (27). We denote $\mathcal{R}_{\text{asy},\,h}(L)$, $\mathcal{T}_{\text{asy},\,h}(L)$ these approximations. The results are given in Figures 8 right and 9 right. We observe that the curves are in good agreement, that is $\mathcal{T}_h$ (resp. $\mathcal{R}_h$) and $\mathcal{T}_{\text{asy},\,h}(L)$ (resp. $\mathcal{R}_{\text{asy},\,h}(L)$) are close to each other. Figure 10, where the errors $L \mapsto |\mathcal{T}_h - \mathcal{T}_{\text{asy},\,h}(L)|$ and $L \mapsto |\mathcal{R}_h - \mathcal{R}_{\text{asy},\,h}(L)|$ are displayed, confirms this impression. Errors are small even though L is not that large. This is due to exponential convergence with respect to L. Actually on Figure 10, we observe that rapidly the numerical error becomes predominant with respect to the asymptotic error as L increases.

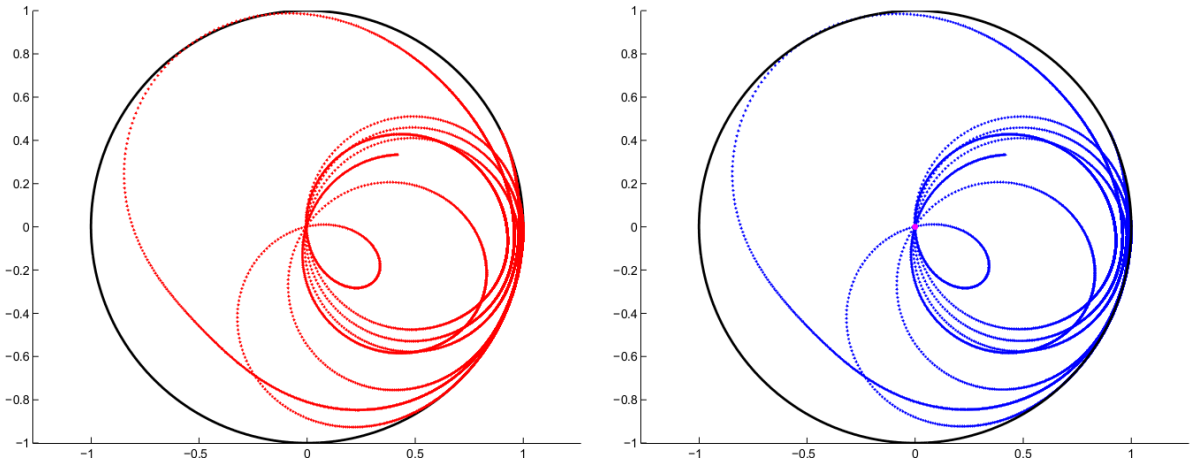

Figure 8: Coefficients $\mathcal{T}_{L,\,h}$ (left) and $\mathcal{T}_{\text{asy},\,h}(L)$ (right) for $\ell = 1.4 \in (\pi/k;2\pi/k)$ and $L \in (2;10)$.

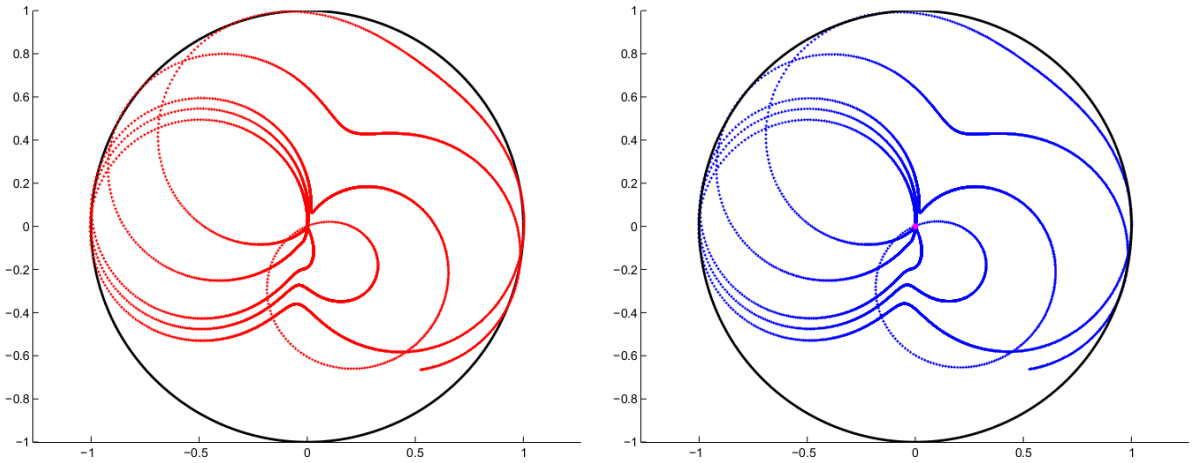

Figure 9: Coefficients $\mathcal{R}_{L,\,h}$ (left) and $\mathcal{R}_{\mathrm{asy},\,h}(L)$ (right) for $\ell = 1.4 \in (\pi/k; 2\pi/k)$ and $L \in (2; 10)$.

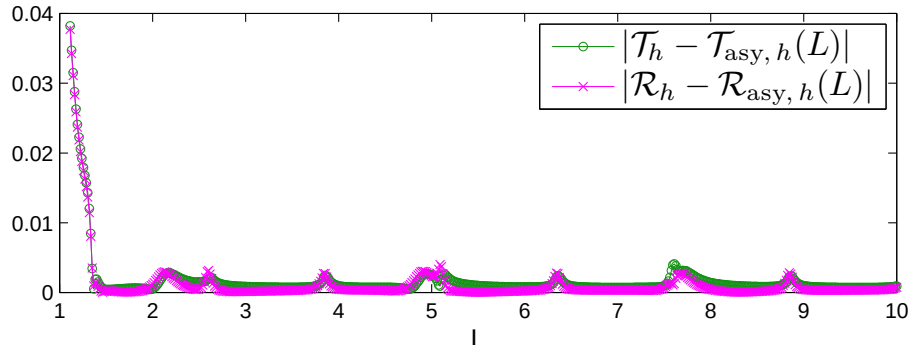

Figure 10: Curves $L \mapsto |\mathcal{T}_h - \mathcal{T}_{\mathrm{asy},\,h}(L)|$ and $L \mapsto |\mathcal{R}_h - \mathcal{R}_{\mathrm{asy},\,h}(L)|$ for $\ell = 1.4$.

In Figure 11, we display the behaviour of the curves $\{\mathcal{T}_{\mathrm{asy}}(L)\,|\,L \in (1; +\infty)\}$ and $\{\mathcal{R}_{\mathrm{asy}}(L)\,|\,L \in (1; +\infty)\}$ for several particular values of the width ℓ of the vertical branch of the waveguide. More precisely, we choose ℓ such that

$$k = m\alpha \qquad \Leftrightarrow \qquad \ell = \frac{\pi}{k}\,\frac{m}{\sqrt{m^2 - n^2}}.$$

with $m = 2, 3, 4, 5$. In (28), we showed that in this case, $\{\mathcal{T}_{\mathrm{asy}}(L)\,|\,L \in (1; +\infty)\}$ and $\{\mathcal{R}_{\mathrm{asy}}(L)\,|\,L \in (1; +\infty)\}$ must be close curves in the complex plane. Our simulations are in accordance with this result.

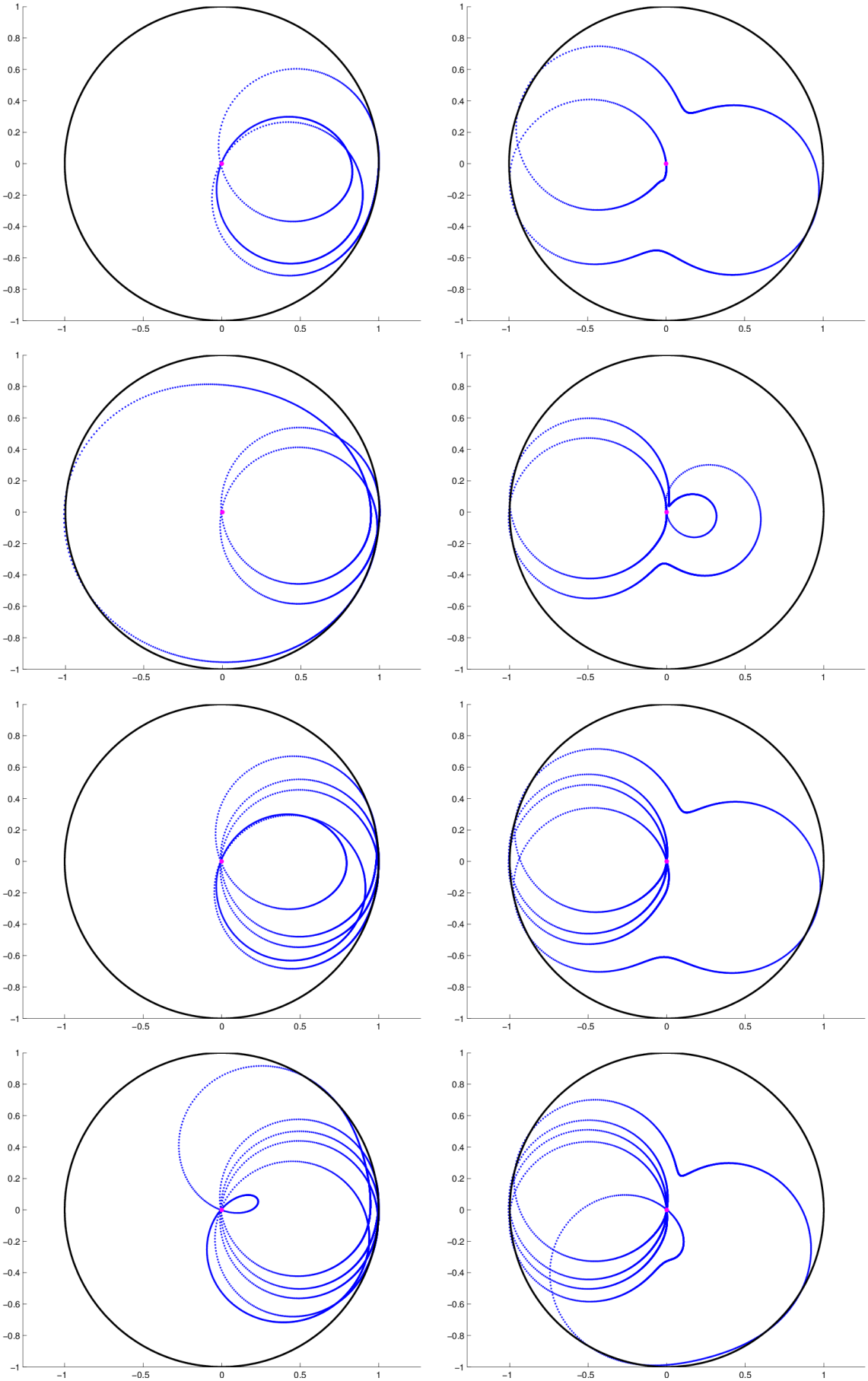

Figure 11: Curves $\{\mathcal{T}_{\mathrm{asy},h}(L)\,|\,L\in(1;+\infty)\}$ (left) and $\{\mathcal{R}_{\mathrm{asy},h}(L)\,|\,L\in(1;+\infty)\}$ (right) for several values of $\ell\in(\pi/k;2\pi/k)$. For the line $m-1$, $m=2,3,4,5$, we take $\ell=m\pi/(k\sqrt{m^2-1})$.

In Figure 12, we represent the numerical approximation of the curves $\{\mathcal{T}_{\text{asy}}(L)\,|\,L \in (2;200)\}$ and $\{\mathcal{R}_{\text{asy}}(L)\,|\,L \in (2;200)\}$ for $\ell = 1.7$. We can prove in this case that the ratio k/α is an irrational number. As predicted, the curves goes through zero. It seems also that they fill the unit disk. However, we are not able to prove it.

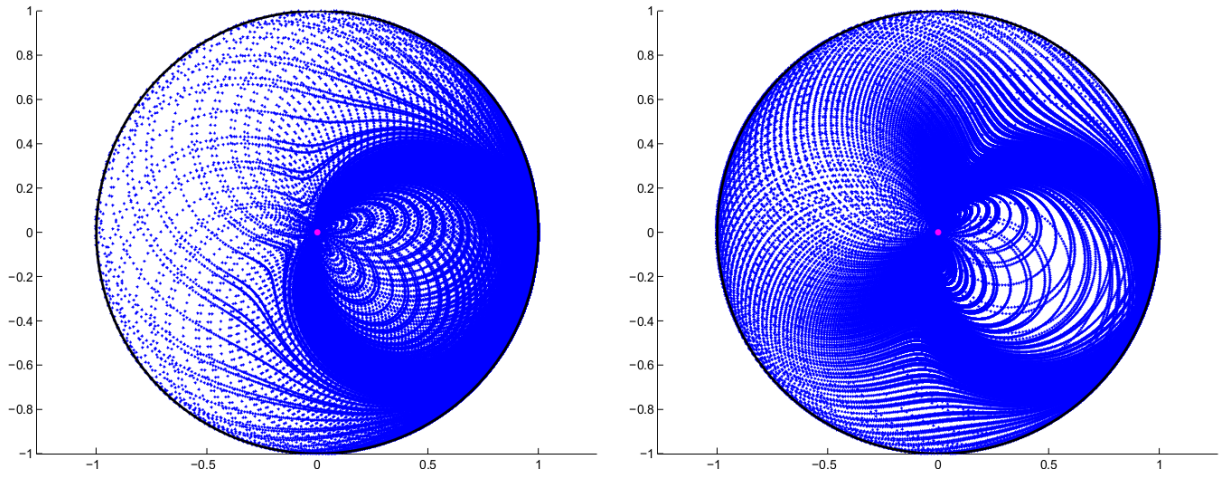

Figure 12: Coefficients $\mathcal{T}_{\text{asy},\,h}(L)$ (left) and $\mathcal{R}_{\text{asy},\,h}(L)$ (right) for $\ell = 1.7 \in (\pi/k; 2\pi/k)$ and $L \in (2;200)$.

7.3 Non-reflectivity

We give examples of waveguides where $\mathcal{R} = 0$ for well-chosen ℓ and L. Numerically we set ℓ and then we compute $\mathcal{R}_h$ for a range of L. Finally, we select the L such that $-\ln|\mathcal{R}_h|$ is maximum.

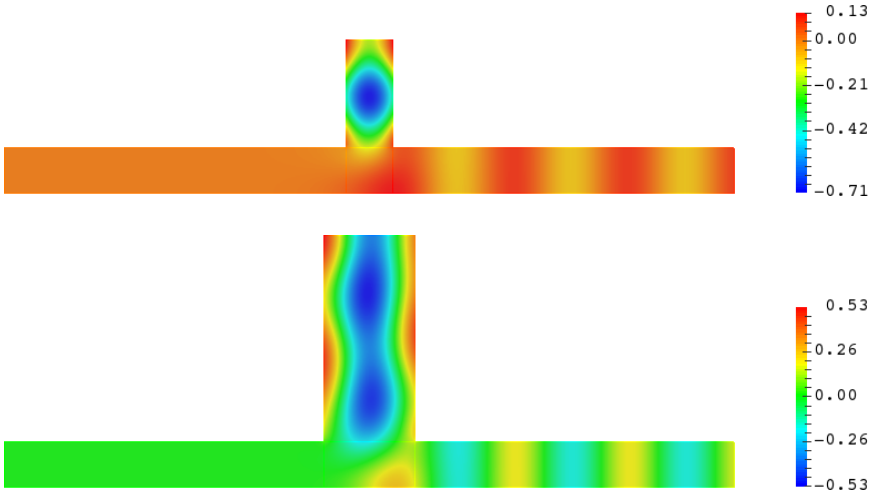

Figure 13: Real part of $v_h - w_h^+$ in geometries where we have non-reflectivity. Top: $\ell = 1 \in (0;\pi/k)$ and $L = 3.3649$ ($\mathcal{R}_h \approx (-7.8 + 8.9i).10^{-6}$). Bottom: $\ell = 2 \in (\pi/k; 2\pi/k)$ and $L = 5.5329$ ($\mathcal{R}_h \approx (1.4 + i).10^{-5}$). As expected, the amplitude of the field is very small at $x = -8$.

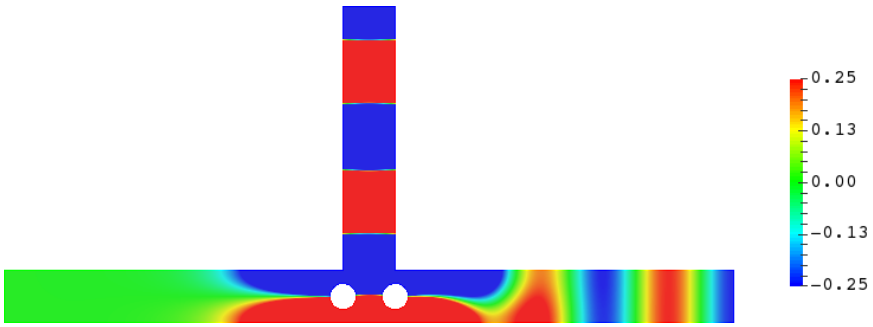

Figure 14: Real part of $v_h - w_h^+$ in another geometry where we have non-reflectivity. The waveguide contains two rather large non penetrable obstacles with Neumann boundary condition. Therefore one would expect that some energy would be backscattered. But due to the presence of the vertical branch whose height has been finely tuned, this is not the case and energy is completely transmitted ($|\mathcal{T}| = 1$).

7.4 Perfect reflectivity

Now, we provide examples of waveguides where $\mathcal{T} = 0$. This time, we select the L such that $-\ln|\mathcal{T}_h|$ is maximum.

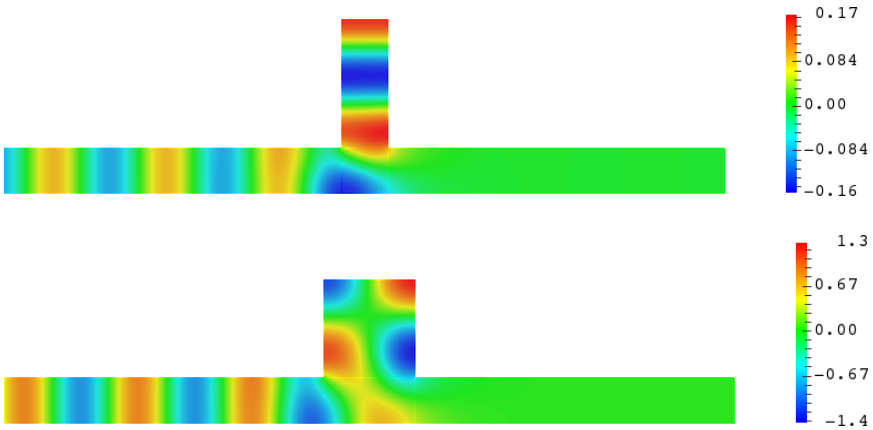

Figure 15: Real part of the total field v_h in geometries where we have perfect reflectivity. Top: $\ell = 1 \in (0;\pi/k)$ and $L = 3.85962$ ($\mathcal{T}_h \approx (-5.3 + 6.1i).10^{-4}$). Bottom: $\ell = 2 \in (\pi/k; 2\pi/k)$ and $L = 3.152073$ ($\mathcal{T}_h \approx (-7.3 + 2.7i).10^{-4}$). As expected, the amplitude of the field is very small at $x = 8$.

7.5 Perfect invisibility

Finally, we show examples of waveguides where $\mathcal{T} = 1$. We start from the domain

$$\Omega_L^\gamma := \{(x,y) \in \mathbb{R} \times (0;1) \ \cup \ (-\ell/2;\ell/2) \times [1;L) \ \cup \ (\pm\vartheta - 1/2; \pm\vartheta + 1/2) \times [1;\gamma).$$

Numerically, first we set $\ell \in (0;\pi/k)$ and $\vartheta = 1.5$ (see the notation in Section 6, Figure 4). Then we approximate the solution of Problem (12) (half-waveguide problem with mixed boundary conditions) for $\gamma \in (1;10)$. We select one $\gamma = \gamma_\infty$ such that $-\ln|R_{\infty,h} + 1|$ is maximum. Thus we impose $R_{\infty,h} \approx -1$. Eventually, we approximate the solution of the initial Problem (2) set in $\Omega_L^{\gamma_\infty}$ for $L \in (5;10)$ and we take L such that $-\ln|\mathcal{T}_h - 1|$ is maximum. We try to cover a range of (relatively) high values of L so that R_h remains close to $R_{\infty,h} \approx -1$. Indeed, we remind the reader that the error $|R - R_\infty|$ is exponentially small as $L \to +\infty$ (see (13)).

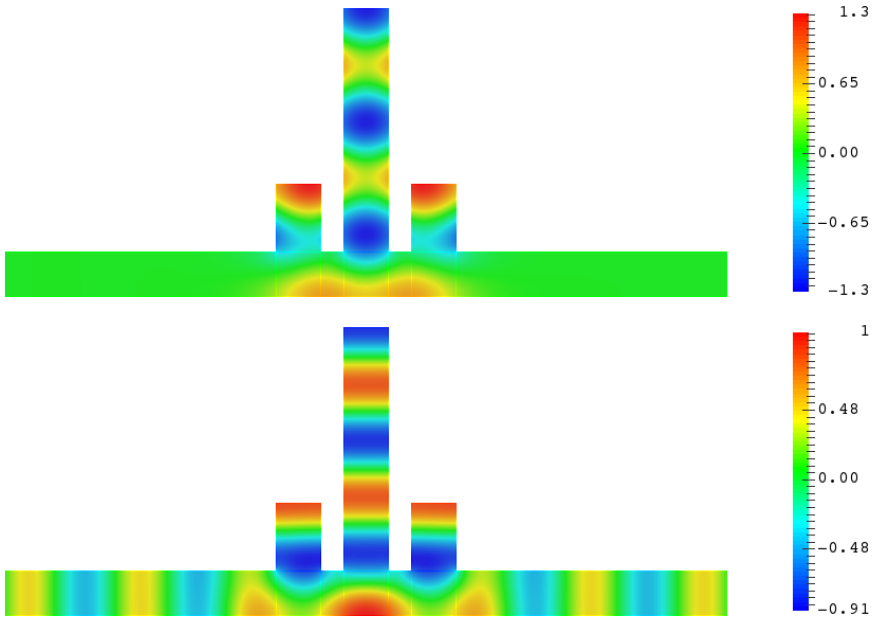

Figure 16: Example of geometry where we have perfect invisibility: $\ell = 1 \in (0; \pi/k)$, $\gamma = 2.4959$, $L = 6.384936$ and $\vartheta = 1.5$. Numerically, we obtain a scattering coefficient $\mathfrak{T}_h$ such that $\mathfrak{T}_h - 1 \approx (-6.5 + 1.4i).10^{-6}$. Top: real part of $v_h - w_h^+$. Bottom: real part of the total field v_h.

8 Conclusion

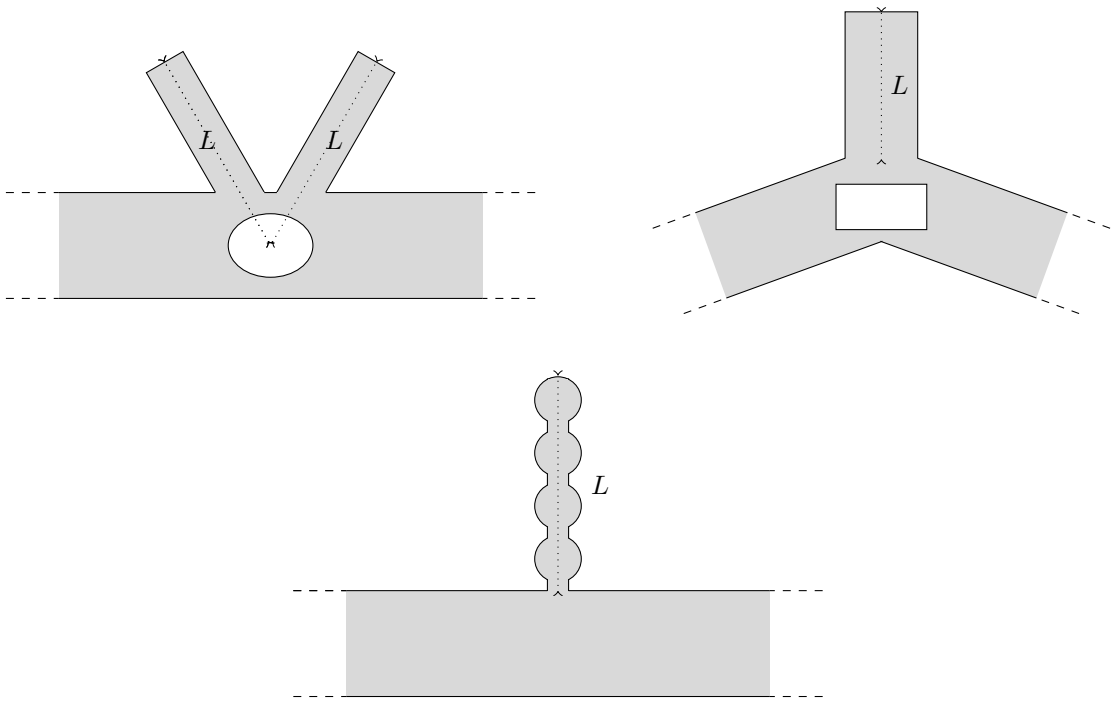

Figure 17: Top: non perpendicular branches. Bottom: periodic vertical branch.

In this article, we have explained how to construct waveguides where non reflectivity ($\mathcal{R} = 0$, $|\mathcal{T}| = 1$), perfect reflectivity ($|\mathcal{R}| = 1$, $\mathcal{T} = 0$) or perfect invisibility ($\mathcal{R} = 0$, $\mathcal{T} = 1$) hold. To proceed, we have worked in geometries which are symmetric with respect to the (Oy) axis and which have one or several vertical branch(es) of finite length. In our presentation, we have always assumed that the branch of finite length is perpendicular to the principal waveguide. Such an assumption is not needed and situations like the ones of Figure 17 top can be considered. We could also investigate settings with truncated periodic waveguides as described in Figure 17 bottom as long as waves can propagate

in the vertical branch. Again we mention that we have considered only 2D problems with Neumann boundary condition but higher dimension with other boundary conditions can be dealt using exactly the same procedure. The analysis we have presented works for the monomode regime ($0 < k < \pi$). It seems complicated to extend it to configurations where several propagating modes exist in the horizontal waveguide.

Acknowledgments

The research of S.A. N. was supported by the grant No. 15-01-02175 of the Russian Foundation on Basic Research. V. P. acknowledges the financial support of the Agence Nationale de la Recherche through the Grant No. DYNAMONDE ANR-12-BS09-0027-01.

References

[1] A. Alù, M.G. Silveirinha, and N. Engheta. Transmission-line analysis of ε-near-zero–filled narrow channels. *Phys. Rev. E*, 78(1):016604, 2008.

[2] A.-S. Bonnet-Ben Dhia, L. Chesnel, and S.A. Nazarov. Non-scattering wavenumbers and far field invisibility for a finite set of incident/scattering directions. *Inverse Problems*, 31(4):045006, 2015.

[3] A.-S. Bonnet-Ben Dhia, L. Chesnel, and S.A. Nazarov. Perfect transmission invisibility for waveguides with sound hard walls. *J. Math. Pures Appl., in press, https://doi.org/10.1016/j.matpur.2017.07.020*, 2017.

[4] A.-S. Bonnet-Ben Dhia, E. Lunéville, Y. Mbeutcha, and S.A. Nazarov. A method to build non-scattering perturbations of two-dimensional acoustic waveguides. *Math. Methods Appl. Sci.*, 40(2):335Ű–349, 2017.

[5] A.-S. Bonnet-Ben Dhia and S.A. Nazarov. Obstacles in acoustic waveguides becoming "invisible" at given frequencies. *Acoust. Phys.*, 59(6):633–639, 2013.

[6] A.-S. Bonnet-Ben Dhia, S.A. Nazarov, and J. Taskinen. Underwater topography "invisible" for surface waves at given frequencies. *Wave Motion*, 57(0):129–142, 2015.

[7] E. Bulgakov and A. Sadreev. Formation of bound states in the continuum for a quantum dot with variable width. *Phys. Rev. B*, 83(23):235321, 2011.

[8] G. Cardone, S.A. Nazarov, and K. Ruotsalainen. Asymptotic behaviour of an eigenvalue in the continuous spectrum of a narrowed waveguide. *Sb. Math.*, 203(2):153, 2012.

[9] G. Cattapan and P. Lotti. Bound states in the continuum in two-dimensional serial structures. *Eur. Phys. J. B*, 66(4):517–523, 2008.

[10] L. Chesnel, N. Hyvönen, and S. Staboulis. Construction of indistinguishable conductivity perturbations for the point electrode model in electrical impedance tomography. *SIAM J. Appl. Math.*, 75(5):2093–2109, 2015.

[11] L. Chesnel and S.A. Nazarov. Team organization may help swarms of flies to become invisible in closed waveguides. *Inverse Problems and Imaging*, 10(4):977–1006, 2016.

[12] E.B. Davies and L. Parnovski. Trapped modes in acoustic waveguides. *Q. J. Mech. Appl. Math.*, 51(3):477–492, 1998.

[13] B. Edwards, A. Alù, M.G. Silveirinha, and N. Engheta. Reflectionless sharp bends and corners in waveguides using epsilon-near-zero effects. *J. Appl. Phys.*, 105(4):044905, 2009.

[14] D.V. Evans. Trapped acoustic modes. *IMA J. Appl. Math.*, 49(1):45–60, 1992.

[15] D.V. Evans, M. Levitin, and D. Vassiliev. Existence theorems for trapped modes. *J. Fluid. Mech.*, 261:21–31, 1994.

[16] D.V. Evans, M. McIver, and R. Porter. Transparency of structures in water waves. In *Proceedings of 29th International Workshop on Water Waves and Floating Bodies*, 2014.

[17] M. Fernyhough and D.V. Evans. Full multimodal analysis of an open rectangular groove waveguide. *Trans. Microw. Theory Techn.*, 46(1):97–107, 1998.

[18] R. Fleury and A. Alù. Extraordinary sound transmission through density-near-zero ultranarrow channels. *Phys. Rev. Lett.*, 111(5):055501, 2013.

[19] Y. Fu, Y. Xu, and H. Chen. Additional modes in a waveguide system of zero-index-metamaterials with defects. *Scientific reports*, 4, 2014.

[20] S. Hein, W. Koch, and L. Nannen. Trapped modes and fano resonances in two-dimensional acoustical duct–cavity systems. *J. Fluid. Mech.*, 692:257–287, 2012.

[21] A.I. Korolkov, S.A. Nazarov, and A.V. Shanin. Stabilizing solutions at thresholds of the continuous spectrum and anomalous transmission of waves. *Z. Angew. Math. Mech.*, 96(10):1245–Ű1260, 2016.

[22] C.M. Linton and P. McIver. Embedded trapped modes in water waves and acoustics. *Wave motion*, 45(1):16–29, 2007.

[23] V.G. Maz'ya, S.A. Nazarov, and B.A. Plamenevskiĭ. *Asymptotic theory of elliptic boundary value problems in singularly perturbed domains, Vol. 1.* Birkhäuser, Basel, 2000. Translated from the original German 1991 edition.

[24] N. Moiseyev. Suppression of Feshbach resonance widths in two-dimensional waveguides and quantum dots: a lower bound for the number of bound states in the continuum. *Phys. Rev. Lett.*, 102(16):167404, 2009.

[25] S.A. Nazarov. Sufficient conditions on the existence of trapped modes in problems of the linear theory of surface waves. *J. Math. Sci.*, 167(5):713–725, 2010.

[26] S.A. Nazarov. Trapped modes in a T-shaped waveguide. *Acoust. Phys.*, 56(6):1004–1015, 2010.

[27] S.A. Nazarov. Asymptotic expansions of eigenvalues in the continuous spectrum of a regularly perturbed quantum waveguide. *Theor. Math. Phys.*, 167(2):606–627, 2011.

[28] S.A. Nazarov. Eigenvalues of the Laplace operator with the Neumann conditions at regular perturbed walls of a waveguide. *J. Math. Sci.*, 172(4):555–588, 2011.

[29] S.A. Nazarov. Trapped waves in a cranked waveguide with hard walls. *Acoust. Phys.*, 57(6):764–771, 2011.

[30] S.A. Nazarov. Enforced stability of an eigenvalue in the continuous spectrum of a waveguide with an obstacle. *Comput. Math. and Math. Phys.*, 52(3):448–464, 2012.

[31] S.A. Nazarov. Enforced stability of a simple eigenvalue in the continuous spectrum of a waveguide. *Funct. Anal. Appl.*, 47(3):195–209, 2013.

[32] S.A. Nazarov. Scattering anomalies in a resonator above thresholds of the continuous spectrum. *Mat. sbornik.*, 206(6):15–48, 2015. (English transl.: Sb. Math. 2015. V. 206. N 6. P. 782–813).

[33] S.A. Nazarov and B.A. Plamenevskiĭ. *Elliptic problems in domains with piecewise smooth boundaries*, volume 13 of *Expositions in Mathematics*. De Gruyter, Berlin, Germany, 1994.

[34] S.A. Nazarov and A.V. Shanin. Calculation of characteristics of trapped modes in t-shaped waveguides. *Computational Mathematics and Mathematical Physics*, 51(1):96–110, 2011.

[35] S.A. Nazarov and J.H. Videman. Existence of edge waves along three-dimensional periodic structures. *J. Fluid. Mech.*, 659:225–246, 2010.

[36] V.C. Nguyen, L. Chen, and K. Halterman. Total transmission and total reflection by zero index metamaterials with defects. *Phys. Rev. Lett.*, 105(23):233908, 2010.

[37] A. Ourir, A. Maurel, and V. Pagneux. Tunneling of electromagnetic energy in multiple connected leads using ε-near-zero materials. *Opt. Lett.*, 38(12):2092–2094, 2013.

[38] R. Porter and J.N. Newman. Cloaking of a vertical cylinder in waves using variable bathymetry. *J. Fluid Mech.*, 750:124–143, 2014.

[39] F. Ursell. Trapping modes in the theory of surface waves. *Proc. Camb. Philos. Soc.*, 47:347–358, 1951.

[40] L.A. Vainshtein. Diffraction theory and the factorization method. *Sov. Radio, Moscow*, 1966. (Russian).